Biosensors and Bioelectronics 129 (2019) 15–23

Contents lists available at ScienceDirect

Biosensors and Bioelectronics

journal homepage: www.elsevier.com/locate/bios

A wearable origami-like paper-based electrochemical biosensor for sulfur mustard detection

Noemi Colozza[a], Kai Kehe[b,d], Giulio Dionisi[a], Tanja Popp[c,d], Amelie Tsoutsoulopoulos[c], Dirk Steinritz[c,d], Danila Moscone[a], Fabiana Arduini[a,*]

[a] Department of Chemical Science and Technologies, University of Rome Tor Vergata, Via della Ricerca Scientifica, 00133 Rome, Italy
[b] Bundeswehr Medical Academy, Medical CBRN Defence, Munich, Germany
[c] Bundeswehr Institute of Pharmacology and Toxicology, Munich, Germany
[d] Walther-Straub-Institute of Pharmacology and Toxicology, Ludwig-Maximilian-University Munich, Munich, Germany

ARTICLE INFO

Keywords:
Screen-printed electrode
Prussian blue nanoparticles
Carbon black
Chemical warfare agents
Choline oxidase inhibition

ABSTRACT

The synthesis and employment of volatile toxic compounds as chemical weapons with a large-scale destructive power has introduced a new insidious threat over the last century. In this framework, the development of wearable sensing tools represents a critical point within the security field, in order to provide early alarm systems. Herein, a novel wearable electrochemical biosensor was developed for the rapid and on-site detection of mustard agents. Since a chemical attack is typically carried out by spraying these volatile agents into air, the sensor was designed in order to be able to measure mustard agents directly in the aerosol phase, further than in the liquid phase. The electrodes were screen-printed onto a filter paper support, which allowed to harness the porosity of paper to pre-load all the needed reagents into the cellulose network, and hence to realise an origami-like and reagent-free device. Mustard agent detection was carried out by monitoring their inhibitory effects toward the choline oxidase enzyme, through the amperometric measurement of the enzymatic by-product hydrogen peroxide. A carbon black/Prussian blue nanocomposite was used as a bulk-modifier of the conductive graphite ink constituting the working electrode, allowing for the electrocatalysis of the hydrogen peroxide reduction. After having verified the detecting capability toward a mustard agent simulant, the applicability of the resulting origami-like biosensor was demonstrated for the rapid and real-time detection of real sulfur mustard, obtaining limits of detection equal to 1 mM and 0.019 g·min/m^3 for liquid and aerosol phase, respectively.

1. Introduction

The interest within the sensor research field in improving the performances of electrochemical sensor, as well as in developing innovative approaches for their application, has been considerably grown over the last years. The recent introduction of miniaturised and wearable support for the development of electrochemical sensors has enlarged the fields of applicability of such analytical tools (Bandodkar et al., 2015, 2016; Gao et al., 2016; Liu et al., 2018). A particularly worthy of note application field is the defence field, in which the versatility and the manageability are crucial characteristics for realising effective real-time warning systems. Indeed, the increasing criticality of the ongoing terrorist activity have generated growing demands for innovative portable and ready-to-use sensing tool, able to monitor the local environment and to identify potential hazards and threats for bystanders.

Wearable sensing devices can fulfil these specific requirements. However, the challenges concerning the realisation of a wearable sensor, typically represented by physical flexibility and adaptability, biocompatibility, low invasiveness, and the availability of strain-resistant detection transducers, make its development a demanding task. In fact, only few examples of devices based on a variety of versatile and wearable supports have been recently introduced in the security field (Cánovas et al., 2016; Mishra et al., 2017a, 2017b, 2018; Chuang et al., 2010).

Within this context, paper represents a suitable support for the development of ad hoc designed wearable electrochemical sensing devices (Adkins and Henry, 2015; Cate et al., 2014; Liana et al., 2012; Nery and Kubota, 2013), thanks to the simplicity of handling, the cost-effectiveness, and the major eco-sustainability in comparison with other classical supports. Furthermore, the cellulose porosity allows for designing instrument-free microfluidic paper-based analytical devices

* Corresponding author.
E-mail address: fabiana.arduini@uniroma2.it (F. Arduini).

https://doi.org/10.1016/j.bios.2019.01.002
Received 16 November 2018; Received in revised form 30 December 2018; Accepted 5 January 2019
Available online 08 January 2019
0956-5663/

(μPADs), by exploiting the capillary forces (Martinez et al., 2007; Cinti et al., 2016; Cinti et al., 2017; Colozza et al., 2018; Dungchai et al., 2011; Abe et al., 2008; Martinez et al., 2007, 2010). In addition, paper can be easily disposed (i.e. by incineration), which represents a strategic characteristic especially for defence field applications, allowing for sustainable decontamination procedures and waste management. A further noteworthy aspect of paper use in the sensor field is represented by its suitability to be employed as a support to realise origami-like systems, in which different layers of paper are overlapped by folding or stacking to obtain a controlled interaction pathway through a 3D configuration (Arduini et al., 2018; Rattanarat et al., 2014). In details, the semipermeable structure of paper can be exploited to realise ready-to-use reagent-free sensors by the easy integration of all reagents required for the sensing process inside the cellulose network, without the need of any immobilising step (Nery and Kubota, 2013; Liu and Crooks, 2011; Li et al., 2016; Wang et al., 2013; Arduini et al., 2018).

In this work, we have exploited the unique advantages of paper-based origami-like devices for the realisation of a wearable, ready, and easy-to-use electrochemical PAD (origami-ePAD) for the early on-site detection of ones among the most dangerous and extensively used chemical warfare agents (CWAs) of the last century: mustard agents (MAs) (Fig. 1). These compounds include sulfur-based agents (bis(2-chloroethyl)sulfide, also known as sulfur mustard (SM) or Yperite), and nitrogen-based agents (bis(2-chloroethyl)ethylamine and bis(2-chloroethyl)methylamine, also known as HN1 and HN2, respectively) (Haines and Fox, 2014; Kehe and Szinicz, 2005; Roshan et al., 2013; Rowell et al., 2009; Steinritz et al., 2007). MAs are used in the war field as chemical weapons, which are typically sprayed into air, generating a highly toxic chemical mist. The lab-based classical detection methods (Hill and Martin, 2002; Kangas et al., 2017) for MAs detection are not suitable for the continuous and real-time monitoring of such compounds during chemical attacks. Few studies have been carried out to develop optical and electrochemical sensors for a faster and easier detection of MAs liquid samples, as summarised in our previous work (Colozza et al., 2018). Nevertheless, there is a necessity of portable and wearable sensors able to detect the presence of the real SM in a chemical mist. In Table 1 we report the summary of sensing systems that are suitable for this task, in order to highlight the lack of examples in literature that can adequately fulfil the required needs.

An alternative approach is based on enzymatic amperometric bioassay exploiting the MAs inhibitory activity toward choline oxidase enzyme (ChOx) (Barron et al., 1948a, 1948b), as previously reported by our group using miniaturised screen-printed electrodes (SPEs) realised on polyester (Arduini et al., 2015) and office paper support (Colozza et al., 2018). In these studies, SPEs were modified by drop-casting with Prussian blue-based dispersion to enhance the electrochemical performances of H_2O_2 detection (ChOx enzymatic by-product), thanks to the well-known Prussian blue electrocatalytic properties toward the reduction of H_2O_2 (Cinti et al., 2014; Kubesa et al., 2014; Ricci and Palleschi, 2005). Harnessing the principle of this enzymatic bioassay, in the present work we realised the first wearable biosensor for the on-site detection of airborne MAs. We used filter paper support to design a 3D-structured filter paper-based origami-ePAD, consisting in a three-electrode printed cell (first origami layer) and a filter paper PAD (second origami layer). In order to simplify and speed up the sensor production, a graphite ink modified with a carbon black/Prussian blue nanocomposite (CB/PBNPs) was employed for the printing of the working electrode. The reagents needed for the analysis were pre-loaded by adsorption onto separate areas of the origami, obtaining a sensor "ready-to-use" without the necessity of additional reagents for the analysis. Then the measurements were carried out by assembling the origami layers, allowing for the reaction within the pre-loaded reagents. The ePAD inhibition monitoring capacity was firstly tested by using a lesser toxic MAs simulant, (bis-(2-chloroethyl) amine), and subsequently the origami-ePAD was applied to detect the real SM in the compliance with the appropriate security measures at the Bundeswehr Institute of Pharmacology and Toxicology (Munich, Germany). SM measurements were carried out in the liquid phase as well as in the aerosol form, obtained by spraying SM standard solutions into a tailored sealed flow system with a nebuliser, in order to demonstrate the applicability of the developed sensing tool both for contaminated liquids and for the on-site monitoring of SM-containing mist.

2. Materials and methods

2.1. Reagents and instrumentations

KH_2PO_4 and KCl 100 mM from Carlo Erba were used to prepare phosphate buffer 50 mM. CB/PBNPs powder was synthesised by using $K_3Fe(CN)_6$ and HCl 37% (w/w) obtained from Sigma, and $FeCl_3$ from Fluka·H_2O_2 30% (w/w) and paraoxon were purchased from Sigma-Aldrich, while Choline Chloride and Choline Oxidase (from *Alcaligenes* sp.) and the nitrogen mustard simulant bis(2-chloroethyl) amine were obtained from Sigma. Lead and arsenic standard solutions were purchased from Carlo Erba. Sulfur mustard (purity > 99% confirmed by NMR) was synthesised by the TNO (The Hague, The Netherlands) and

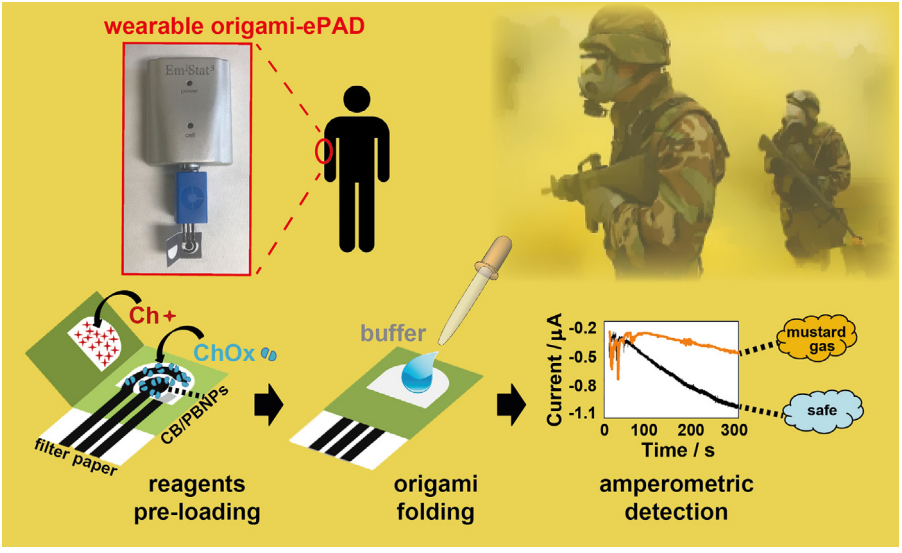

Fig. 1. Working principle of the herein developed wearable origami-ePAD.

Table 1
Main analytical sensing devices reported in literature for mustard agent detection in vapour/gas/aereosol phase.

Principle of detection	Sensitive component	Analyte detected	Analytical performances	Wearability/ portability	Ref.
Automated chemical agent detector based on Surface Acoustic Wave (SAW) sensors.	Chemoselective functionalised polymer, tailored for the vapour phase detection of specific CWAs.	**SM** (bis(2-choloroethyl) sulfide) in vapour phase.	LOD = 80 ppb (real-time analysis).	Portable but not wearable	McGill et al. (2000)
Binary channel Surface Acoustic Wave (SAW) piezoelectric chip.	Sensitive film composed by $PdPc_{0.3}PANI_{0.7}$ (phthalocyanine palladium (PdPc), polyaniline (PANI) and a little dopant with mixing ratio of 3:7).	Mustard agents in gas phase.	Linear range up to 7 mg/m^3. Response time = 5 min	Not discussed.	Shi et al. (2006).
Polymer-coated piezoelectric quartz crystal microbalance (PC-QCM).	Epoxy resin (diglycidyl ether of bisphenol A and epichlorohydrin monomers).	**SM** (bis(2-choloroethyl) sulfide) in vapour phase.	A single concentration of 155 ppm. Response time = 60 s	Not portable or wearable	Bunkar et al. (2010).
Chromogenic and fluorogenic Detection using squaraine dye.	A dithiol, sensitive to SM, able to quench squaraine dye in absence of SM.	Mustard simulant (2-choloroethyl ethyl sulfide) in solid support (filter paper), soil and vapour phase.	LOD = 50 μM and 10 μM by visual and fluorescence methods, respectively. Response time: the detection require the addition of the dye after the dithiol exposure to MAs, for generating the colorimetric response.	Not discussed.	Kumar and Anslyn (2013).
Enzyme inhibition electrochemical sensor, based on a screen-printed origami-like ePAD.	ChOx enzyme.	Mustard simulant (bis(2-chloroethyl) amine) and **SM** (bis(2-choloroethyl) sulfide) in aereosol phase.	Mustard simulant: linear range up to 6 mM, LOD = 1 mM. SM: LOD = 19 mg/m^3. Response time = 60 s	Both portable and wearable.	This work

made available by the German Ministry of Defence.

All the electrochemical measurements were performed by means of a portable potentiostat, EmStat^3 (Palm Instrument, The Netherlands), connected to a personal computer (Fig. S1).

A commercially available nebuliser (eFlow rapid nebuliser system, PARI Pharma, Germany) was used to aerosolise the liquid samples to simulate the spreading of SM into air during a chemical attack.

2.2. Paper-based screen-printed electrode preparation

Filter paper-based screen-printed electrodes (SPEs) were home-produced, by following the procedure optimized as reported within previous works (Cinti et al., 2016, 2017a). Filter paper sheets were firstly modified with an ad hoc designed wax pattern, as reported previously (Colozza et al., 2018), in order to delimitate the hydrophilic area in which liquid samples were dropped, avoiding them to reach the electrical contacts through capillary permeation. Wax pattern was printed onto filter paper (67 g/m^2, Cordenons, Italy) by means of a ColorQube 8580 Xerox printer, and treated at 100 °C for 2 min in order to allow the wax to homogeneously permeate through paper network. Then, conductive inks were used to print a three-electrode system onto wax-modified filter paper sheets, by employing a 245 DEK (Weymouth, UK) serigraphic printer. The conductive inks were applied through masks with the desired patterns. The working and counter-electrodes were obtained using a CB/PBNPs-modified graphite-based ink (Electrodag Loctite 423 SS) and the pseudo-reference electrode was printed using Ag/AgCl-based ink (Electrodag Loctite 6033 SS), both purchased from Henkel. Before printing, the graphite-based ink was modified with a powder of CB/PBNPs prepared as reported by Cinti at al., 2014 and by mixing 0.5 g of CB/PBNPs powder with 9.5 g of graphite ink. The resulting SPEs showed a working electrode area of 0.1256 cm^2.

2.3. Reagents pre-loading and amperometric measurement of H_2O_2

The reagents were trapped into the paper cellulose network through a pre-loading step and stored until the sensor utilisation. In details, two kinds of sensors were used: a one-layer ePAD, constituted only by the filter paper SPEs, and a two-layer origami-ePAD, constituted by the filter paper SPE combined with a wax-modified filter paper PAD. All the solutions were daily prepared in phosphate buffer 50 mM + KCl 100 mM, pH = 7.4 and dropped onto the hydrophilic area delimited by wax. Different combinations of the reagents pre-loading were employed, as described below.

2.3.1. One-layer ePAD

This sensor configuration was used for the preliminary studies. First of all, direct measurement of H_2O_2 was carried out by adding 5 μL of H_2O_2 solutions at several concentrations (from 0.1 to 10 mM) onto the back of the paper-based sensor. Afterward, the sensor was used to detect H_2O_2 by-product of the Ch/ChOx enzymatic reaction. 5 μL of Ch solutions at different concentrations (from 0.1 to 20 mM) were pre-loaded onto the back of the one-layer sensor. After the drying process, the detection was carried out by adding 10 μL of a solution of ChOx 1000 mU/mL.

2.3.2. Origami-ePAD

Both Ch and ChOx solutions were separately pre-loaded onto the origami-ePAD. The most performing configuration was obtained by pre-loading 5 μL of Ch solution 20 mM onto the filter paper PAD and 5 μL of ChOx solution 4000 mU/mL onto filter paper SPE. After the drying process, the electrochemical cell was completed by fixing the two layers together with a common glue. Then the enzymatic reaction was activated by adding 20 μL of phosphate buffer solution, in order to carry out the amperometric measurement of H_2O_2 by-product, obtaining the final concentrations of 5 mM and 1000 mU/mL for Ch and ChOx, respectively.

For each sensor design, the measurement of H_2O_2 enzymatic by-product, in presence or in absence of MAs, was carried out with amperometric technique, applying a potential of 0.0 V (vs Ag/AgCl) for 300 s.

2.4. MAs simulant detection

The bis(2-chloroethyl) amine nitrogen mustard simulant was used for the preliminary studies. The measurement was carried out by the amperometric monitoring of H_2O_2 current, which decreased as a consequence of the inhibition activity toward the Ch/ChOx enzymatic reaction (see Section 2.8). For these measurements, one-layer ePAD were used (prepared as described in Section 2.4). A drop of few microliters (from 0.1 to 1.5 μL) of the 100 mM simulant was added onto the front of the filter paper SPE, in order to reach concentrations between 1 and 25 mM, then 10 μL of a ChOx solution 1000 mU/mL were immediately dropped and the amperometric detection was started.

2.5. Sulfur mustard detection in liquid phase

All experiments with SM were carried out at Bundeswehr Institute of Pharmacology and Toxicology (Munich, Germany) in a safe environment. For these measurements, the origami-ePADs were used (prepared as described in Section 2.4). Since SM is very poorly soluble in water, standard solutions of SM were prepared in pure ethanol. In details, prior to fix the two layers of the origami, 1 μL of SM or ethanol was added onto the front side of the SPE layer in order to obtain the electrochemical response in presence and in absence, respectively, of the inhibitory agent. Immediately after the addition of SM, the origami was closed and 20 μL of the phosphate buffer were added in order to carry out the amperometric measurement. Since the final concentration of ethanol in the resulting 20 μL drop was 5% v/v, measurements in absence of SM were carried out by using a mixture of phosphate buffer and ethanol at 5% v/v, in order to obtain a consistent baseline.

2.6. Sulfur mustard detection in aerosol phase

An accurately sealed system for the detection of aerosolised solutions of SM was realised and employed for the amperometric measurements with the origami-ePAD (Fig. S1). Standard solutions were aerosolised by means of a nebuliser (eFlow, PARI Pharma, Germany), hence the resulting aerosol was led into a three-neck bottle and finally into a bottle containing a highly concentrated hypochlorite solution, used for the decontamination of SM. A mixture of phosphate buffer solution and ethanol at 2.5% v/v was used to obtain the baseline responses, as well as to prepare all the SM standard solutions to be aerosolised. In details, 6 mL of solution were added into the nebuliser chamber, which aerosolised them with a flow rate of 0.6 mL/min. Measurements were carried out by introducing the origami-ePAD into the central neck of the three-neck bottle. The sensor cable was fixed onto a metallic rod, in order to minimise the movements of the sensor and the consequent electrical noise generation. The entire system was used under a safety hood, in order to prevent the risk of possible leaks.

The exposure to the aerosolised SM was carried out simultaneously with the amperometric measurement, for a period of 5 min, using concentrations of 0.019, 0.19 and 0.76 g/m^3.

2.7. Inhibition percentage calculation

The inhibition extent was calculated from the difference between the amperometric response obtained in presence and in absence of the inhibitory agent, at constant conditions and Ch/ChOx concentrations. The inhibition percentage (*I%*) was hence calculated as reported in the following equation:

$$I\% = \frac{I_0 - I}{I_0} \cdot 100$$

where I_0 and I are the current intensities corresponding to H_2O_2 produced by the enzymatic reaction in the absence and in the presence of the simulant, respectively. Current intensities were recorded at the end of the amperometric measurement (t = 300 s) or at different times of the measurement, where specified.

2.8. Safety indications

Safety measures were adopted during the detection and the preparation of SM samples. In details, the measurements of SM were carried out in Bundeswehr Institute of Pharmacology and Toxicology (Munich, Germany). Adequate personal protective equipment was used, and all the instrumentation and needed materials were employed and stored inside a fume hood and afterward decontaminated by using a highly concentrated hypochlorite solution.

3. Results and discussions

The development of the 3D structured origami-ePAD by using wax-modified filter paper as support has been carried out through a stepwise study, in order to understand the effects related to each component of the origami system. In detail, we firstly verified the efficiency of the filter paper properties for our purpose by studying the suitability of ePAD for H_2O_2 enzymatic by-product monitoring in absence and in presence of MAs simulant. Differently from our previous works (Arduini et al., 2015; Colozza et al., 2018), the properties of filter paper support allowed us to design a reagent-free electrochemical biosensor, in which the biological reagents were pre-integrated onto the sensor, also suitable for the detection of airborne aerosolised SM. This characteristic represents a crucial advantage with respect the polyester-based and office paper-based electrochemical sensors.

In the first part of the work, the ePAD was realised by pre-loading only the substrate choline (Ch) onto a CB/PBNPs-based SPE, while choline oxidase solution (ChOx) was added at the moment of the measurement, which represented the first step toward the realisation of a fully-integrated reagent-free biosensor. Subsequently, the origami-ePAD was developed, by pre-loading both ChOx and Ch onto two separated origami layers to deliver a fully-integrated origami-ePAD for the detection of both liquid and aerosolised SM.

3.1. One-layer ePAD: H_2O_2 amperometric detection

Firstly, the suitability of the filter paper-based ePAD for the amperometric detection of H_2O_2 was evaluated by testing its electroanalytical performances. The use of a bulk-modified graphite-based ink by the incorporation of CB/PBNPs nanocomposite allowed for obtaining a printed sensor with intrinsic electrocatalytic properties toward the reduction of H_2O_2. In order to verify the electrocatalytic properties of the CB/PBNPs-modified ink, the H_2O_2 amperometric measurement was investigated in the potential range between – 100 mV and + 100 mV. The study was carried out by adding 5 μL of H_2O_2 1 mM onto the filter paper SPE. The best results in terms of current intensity and repeatability were obtained for an applied potential of 0.0 V, which was chosen for the further studies (Fig. 2A).

Hence, the sensor response was examined for increasing concentration of H_2O_2, obtaining a linear range between 0.1 and 10 mM, described by the equation $y = (0.58 \pm 0.02)x + (0.17 \pm 0.09)$, $r^2 = 0.9956$ (Fig. 2B). Current intensities were sampled at t = 120 s, since the amperogram signals appeared to be stable after this time. Sensitivity, calculated as the ratio between the slope of the regression equation and the working electrode surface area, resulted equal to 4.6 $\mu A\, mM^{-1}\, cm^{-2}$, which is generally lower than the sensitivity reported for the H_2O_2 PB-based detection with other electrochemical

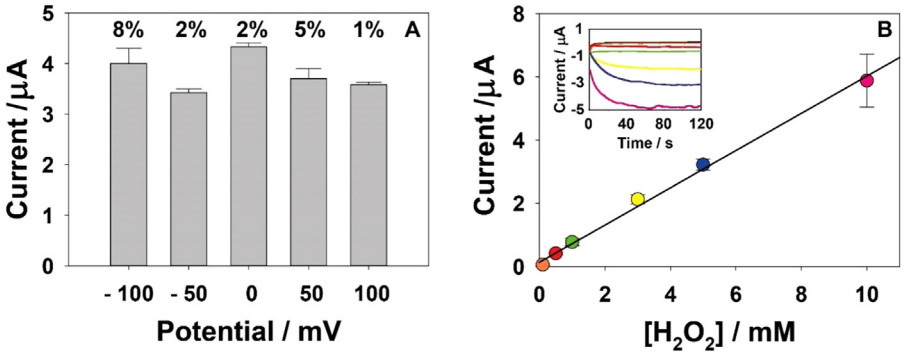

Fig. 2. A) Current intensities (n = 3) recorded from amperometric detection of 5 µL H_2O_2 1 mM at different applied potentials. RSD% is reported for each potential. **B)** Calibration curve (n = 3) obtained with 5 µL of H_2O_2 0.1 mM (orange), 0.5 mM (red), 1 mM (green), 3 mM (yellow), 5 mM (blue), 10 mM (pink), applying E = 0.0 V. Currents in plot are reported as absolute values. Samples were prepared in phosphate buffer 50 mM + 0.1 M KCl (pH = 7.4). Inset: corresponding amperograms. (For interpretation of the references to color in this figure legend, the reader is referred to the web version of this article).

sensors (Cinti et al., 2014; Kubesa et al., 2014; Ricci and Palleschi, 2005). This evidence is consistent with the porous nature of the filter paper support, which determines diffusion processes through the cellulose network of the paper-based SPE (Cinti et al., 2017b; Arduini et al., 2017).

3.2. One-layer ePAD: enzymatic reaction monitoring

The one-layer filter paper-based ePAD was hence applied for the measurement of H_2O_2 by-product from the enzymatic reaction of ChOx with the substrate Ch. These preliminary studies were carried out by pre-loading 5 µL of Ch onto the ePAD from the back side (as further explained in Section 3.4). Then, the amperometric measurement of the enzymatic by-product H_2O_2 was performed by dropping few microliters of a ChOx solution onto the ePAD.

In order to select the best conditions for H_2O_2 by-product detection, different volumes and concentrations of ChOx solution were tested. As shown in Fig. 3A, volumes of a 0.5 U/mL ChOx solution were used ranging from 5 to 15 µL, obtaining the best current intensity for 10 µL. Hence, this volume was used to study the amperometric response for increasing concentrations of ChOx from 0.25 to 1.5 mU/mL (Fig. 3B). The concentration of 1 U/mL was chosen for the further experiments, since it showed a good compromise between current intensity and low amount of enzyme.

Thus, the enzymatic reaction was studied in the selected conditions, obtaining a Michaelis-Menten curve with a K_M equal to 6.1 ± 0.5 mM. This K_M value is considerably higher than the one obtained in our previous work (K_M = 0.62 ± 0.08 mM) (Colozza et al., 2018), due to diffusion processes within the filter paper cellulose network.

Prior to test the detection efficiency toward SM, the ePAD suitability for the monitoring of the ChOx inhibition in presence of MAs was verified by using a less toxic nitrogen MAs simulant, bis(2-chloroethyl) amine. After Ch pre-loading step, different simulant solutions at known concentrations (from 1 to 25 mM) were dropped onto the Ch pre-loaded one-layer ePAD immediately before the ChOx solution for starting the amperometric measurement. As reported in Fig. 4, an increasing inhibition of the enzymatic activity was observed in the presence of increasing concentrations of the simulant, with a linear correlation between 1 and 12.5 mM, corresponding to the equation y = (5.0 ± 0.3)x + (7 ± 2), r^2 = 0.959. LOD was calculated for I% = 15%, resulting in a value of 1.8 mM, while the value corresponding to the concentration giving the 50% of inhibition (IC_{50}) was found equal to 8.0 mM. These results demonstrated the suitability of the filter paper-based ePAD to be applied for the detection of liquid MAs in the millimolar level. Thus, we focused our efforts to realise a ready-to-use and fully-integrated origami-ePAD for the detection of the more toxic SM, which represents

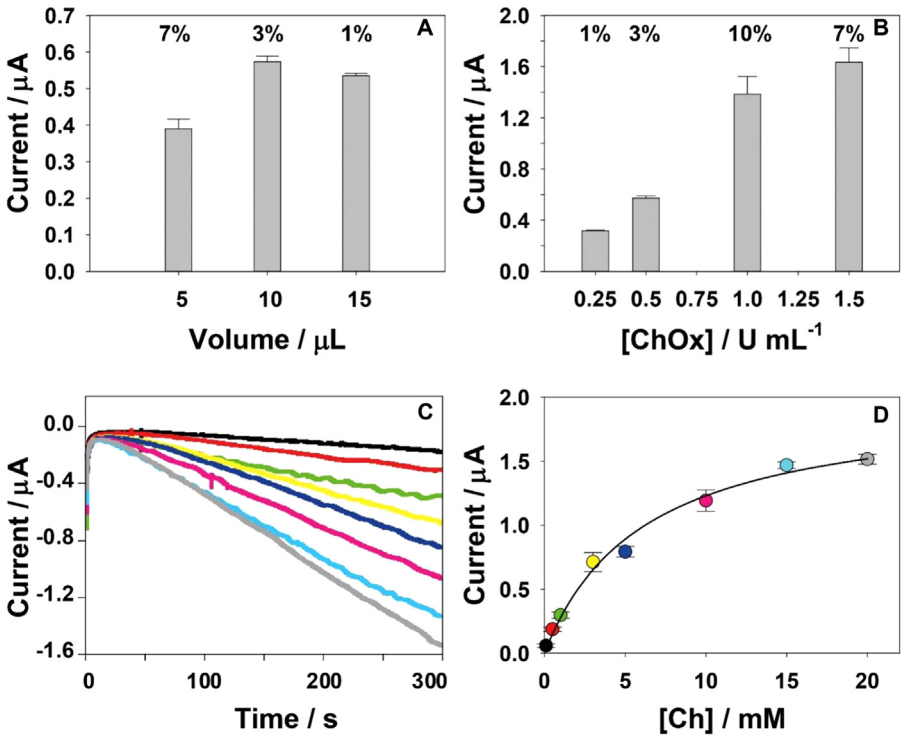

Fig. 3. A) Study of the volume of ChOx solution (using a ChOx concentration of 0.5 U/mL) and **B)** study of the concentration of ChOx solution (using a ChOx volume of 10 µL) (n = 3), obtained from amperometric detection (E = 0.0 V and t = 300 s) of H_2O_2 enzymatic by-product, by using the one-layer ePAD pre-loaded with Ch 5 mM. **C)** Amperograms obtained from the detection (E = 0.0 V and t = 300 s) of H_2O_2 enzymatic by-product obtained with the one-layer ePAD pre-loaded with 5 µL of increasing concentration of Ch: 0.1 mM (black), 0.5 mM (red), 1 mM (green), 3 mM (yellow), 5 mM (blue), 10 mM (pink), 15 mM (light blue), 20 mM (grey), and **D)** corresponding Michaelis-Menten curve (n = 3). Currents in plot are reported as absolute values. Measurements were carried out in phosphate buffer 50 mM + 0.1 M KCl, pH = 7.4. (For interpretation of the references to color in this figure legend, the reader is referred to the web version of this article).

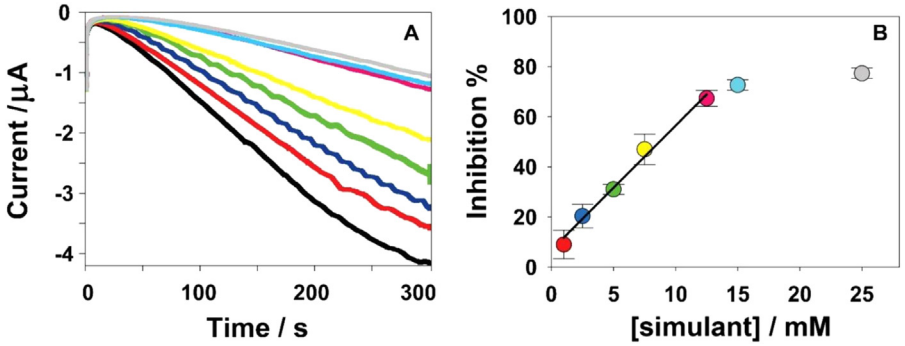

Fig. 4. A) Amperograms obtained from the detection (E = 0.0 V and t = 300 s) of H_2O_2 enzymatic by-product, by using the one-layer ePAD pre-loaded with Ch 5 mM, in absence (black) and in presence of increasing concentrations of MAs simulant (bis(2-chloroethyl) amine): 1 mM (red), 2.5 mM (blue), 5 mM (green), 7.5 mM (yellow), 12.5 mM (pink), 15 mM (light blue), 25 mM (grey). **B)** Corresponding inhibition percentage plot (n = 3). Measurements were carried out in phosphate buffer 50 mM + 0.1 M KCl, pH = 7.4. (For interpretation of the references to color in this figure legend, the reader is referred to the web version of this article).

the major threat within the family of MAs.

3.3. Origami-ePAD: origami settings

In the second part of the work, the two-layer origami-ePAD was designed and developed on the basis of the behaviour observed for the one-layer ePAD. In order to realise the origami sensor, a second layer was added constituting in a wax-printed filter paper PAD, which was fixed together with the SPE-layer by means of a common glue. Starting from the configuration used for the already described one-layer ePAD, different possibilities for the reagent pre-loading step were evaluated. In details, Ch and ChOx solutions were added or pre-loaded according to four different pre-loading configurations, as schematised in Fig. 5A:

1. Ch pre-loaded onto the back side of the SPE (one-layer ePAD);
2. Ch pre-loaded onto the front side of the SPE (one-layer ePAD);
3. Ch pre-loaded onto the front side of the SPE, ChOx pre-loaded onto the PAD (origami-ePAD);
4. ChOx pre-loaded onto the front side of the SPE, Ch pre-loaded onto the PAD (origami-ePAD).

The starting concentration of Ch and ChOx were chosen in order to obtain the final concentration of 5 mM and 1 U/mL, respectively, taking into account the dilution factor that occurred for each configuration. The amperometric measurements of the enzymatic by-product H_2O_2 were carried out by dropping few microliters of a ChOx solution in the case of configurations 1 and 2, while for the configurations 3 and 4 only phosphate buffer solution was needed, since both the enzyme and the substrate were pre-integrated into the origami-ePAD. The resulting amperometric responses were compared to evaluate the effects of the different configurations on the enzymatic kinetic (Fig. 5B). While no significant differences were observed between the configurations 1 and 2 (one-layer ePAD), a sharp decrease of current intensity occurred for the origami-ePAD (configurations 3 and 4). The small difference in the current signals observed between the configurations 1 and 2 (one-layer ePAD) highlighted that the enzymatic reaction is not significantly dependent on Ch solution pre-loading step. Differently, the decreasing of the amperometric response in the cases of the origami-ePAD configurations (3 and 4) showed that the enzymatic kinetic was remarkably delayed when also ChOx was pre-loaded. This evidence can be attributed to the diffusion processes into the cellulose network in which the reagents are loaded. Moreover, it can be noted that the configuration 4 lead to higher current intensity than the configuration 3, suggesting that the effect of diffusion processes onto the enzymatic kinetic is less significant when the enzyme is closer to the electrode surface (configuration 4). In the light of these observations, the configuration 4 was chosen for the realisation of the origami-ePAD for MAs detection.

Successively, several volumes of phosphate buffer solution were used to study the best conditions for amperometric monitoring of the enzymatic reaction with the origami-ePAD. As reported in Fig. 5C and D, a clear influence of the phosphate buffer volume toward the resulting amperometric current was observed. Volumes lower than 10 µL was not

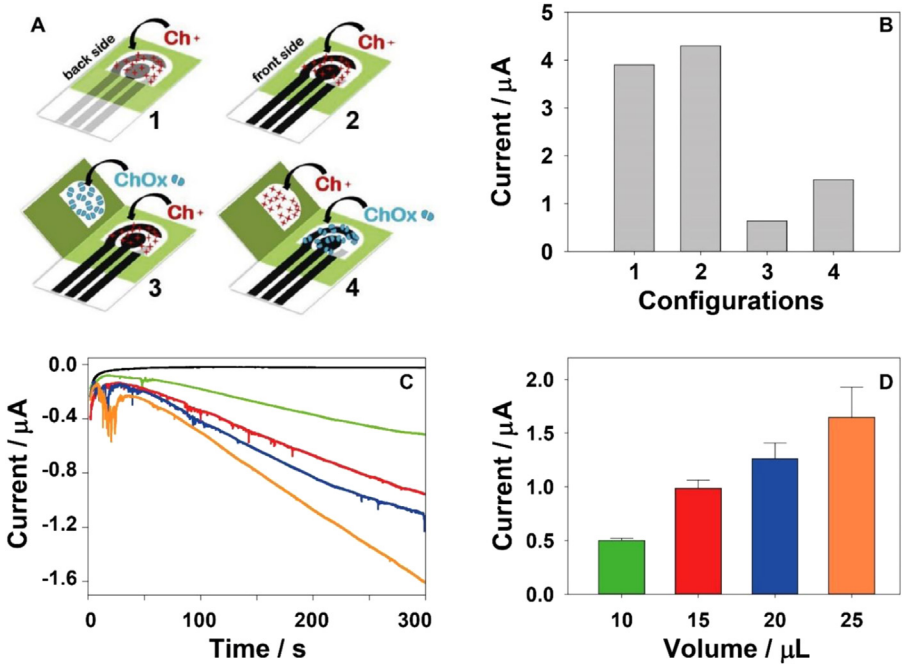

Fig. 5. A) Schematic representation of the one-layer ePADs and origami-ePADs herein realised and **B)** corresponding trend of the current intensities, obtained from the amperometric measurements of the enzymatic by-product H_2O_2. **C)** Amperograms obtained using the origami-ePAD (configuration 4) from the detection (E = 0.0 V and t = 300 s) of H_2O_2 enzymatic by-product by using increasing volumes of phosphate buffer solution: 5 µL (black), 10 µL (green), 15 µL (red), 20 µL (blue) and 25 µL (orange). **D)** Corresponding plot of the current intensities, recorded at t = 300 s, for each phosphate buffer volume (n = 3). Measurements were carried out in phosphate buffer 50 mM + 0.1 M KCl, pH = 7.4, and obtaining a final concentration of Ch and ChOx equal to 5 mM and 1 U/mL, respectively, for each configuration. (For interpretation of the references to color in this figure legend, the reader is referred to the web version of this article).

sufficient to permeate both layers of the origami and to allow for the dissolution and reaction of the reagents, as shown by the very low amperometric signal obtained with 5 µL of phosphate buffer solution (Fig. 5C, black line). The increase of the phosphate buffer volume led to a progressive increase of current intensity and electrical noise. The latter behaviour is probably to be ascribed to aqueous solution diffusion towards electrical contact. Indeed, if large amount of solution is used, the aqueous solution can diffuse overcoming the wax–based zone, with consequently wetting of the electrical contact and noise generation. Furthermore, the significant increase of sensitivity observed for different volumes of phosphate buffer confirmed that the origami-ePAD performances are markedly influenced by the diffusion processes involved for the reagents re-dissolving and reaction. Hence, the volume of 20 µL was chosen, as a good compromise to ensure the efficient re-dissolving of the reagents and, at the same time, to avoid electrical noise.

3.4. Origami-ePAD: detection of liquid SM

The origami-ePAD was thus applied for the detection of standard solutions of SM in liquid phase. SM samples from 1 to 8 mM were prepared in pure ethanol, since the SM solubility in aqueous solution is very low (0.0043 M at 25 °C) (Menger and Elrington, 1991). In order to minimise the inactivation of the enzyme due to presence of ethanol, the amperometric measurements were carried out by analysing 1 µL of SM solution in ethanol, obtaining a ethanol concentration of 5% v/v within the final working solution (i.e. 20 µL of phosphate buffer). Indeed, we have previously pointed out that the condition of 5% v/v of ethanol corresponds to a good compromise between a limited enzyme inactivation and a significant solubilisation of SM (Colozza et al., 2018). A mixture of phosphate buffer and ethanol at 5% v/v was used to obtain the reference amperometric signal in absence of the inhibitory agent (I_0), in order to take into consideration the slight enzyme inactivation occurred in this conditions for the inhibition percentages calculation (as described in Section 2.8).

Hence, SM solutions were dropped on the front side of the SPE layer, facilitating the interactions between the inhibitor and the enzyme. Then, the origami-ePAD was closed and the amperometric measurement was immediately started by the dropping of 20 µL of phosphate buffer solution. As shown in Fig. 6A, a linear range between 1 and 6 mM was obtained, described by the equation $y = (13 \pm 1)x + (15 \pm 6)$, $r^2 = 0.8854$. A LOD value equal to 0.4 mM was calculated for I% = 20%, while IC_{50} was obtained equal to 2.5 mM. The results obtained for the SM detection showed lower IC_{50} and LOD values, as well as an earlier interruption of the linearity trend (which can be observed in the SM inhibition percentage plot, Fig. 6A) with respect to the simulant (Fig. 4), highlighting the higher toxicity of SM.

3.5. Origami-ePAD: detection of aerosolised SM

After having demonstrated the suitability of the developed origami-ePAD for SM detection in liquid phase, a flow analysis system was realised for the detection of aerosolised solution of SM, in order to test the applicability of the developed device for the real-time measurement of airborne SM. The experimental conditions realised for this study was designed to simulate the spread of SM into air during a chemical attack. SM solutions were aerosolised by means of a nebuliser and let flow through a three-neck bottle, in which the biosensor was placed (Fig. S1).

The origami-ePAD was employed for the detection of SM in the aerosolised form, with the aim to apply the ready-to-use sensing tool for the real-time monitoring of SM aerosolised into air. For these experiments, the filter paper PAD layer of the origami was punctured in order to allow the SM aerosol to effectively reach the inner part of the origami and hence promoting its interaction with the enzyme pre-loaded onto the SPE layer. Thus, the origami-ePAD was folded, wet with 20 µL of phosphate buffer solution and introduced into the three-neck bottle. The sensor cable was fixed to a metallic support, in order to minimise the sensor cable oscillation and avoid an excess of electrical noise. The amperometric measurement was thus carried out simultaneously with the exposure to the SM aerosol, for a period of 5 min. With this approach, SM standard solutions down to 0.1 mM were detected, corresponding to aerosol concentrations of 0.019 g/m^3. This concentration is consistent with the level of SM (12–30 mg·min/m^3) which causes only minor ocular irritation (Anderson, 1942). As shown in Fig. 6B, current values were sampled at three times of the resulting amperometric measurement (180 (●) 240 (▼) and 300 (■) s), to evaluate the inhibition extent at different times of exposure. It can be observed that no significant difference can be appreciated among the three different sampling times, confirming the reversible nature of the inhibition mechanism (Arduini et al., 2015). The repeatability of the measurements was evaluated for the concentration of 0.76 g/m^3 at the three sampling times, resulting in RSD% ranging from 6% to 11%. The LOD was calculated for the inhibition occurred after 60 s of exposure, which resulted equal to I% = 10%. As a consequence, we can state that the developed sensing tool is able to alert for the presence of airborne SM in only 60 s. Taking into consideration that the toxic effects of SM are cumulative and hence proportional to the time of exposure to this chemical threat, a very fast detection of airborne SM can represent a vitally important factor, allowing for the immediate warning to the affected bystanders. For instance, a fast detection provides a properly management of the terrorist attack, through the rapid evacuation of the target area and the prompt intervention of medical assistance. Thanks also to the wearability of the origami-ePAD, these observations pave the way for real-time monitoring of SM present in the air by means of an easy and ready-to-use analytical tool, which can be easily disposed after its use.

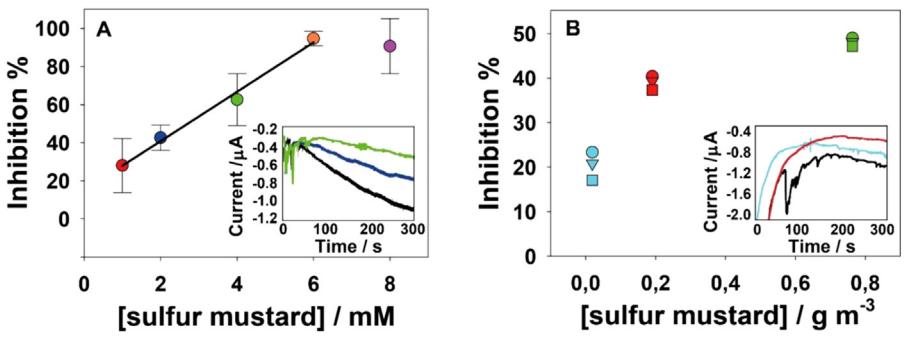

Fig. 6. Results obtained for sulfur mustard (SM) detection by using the origami-ePAD. **A)** Inhibition percentage values (n = 3) for increasing concentrations of liquid SM: 1 mM (red), 2 mM (blue), 4 mM (green), 6 mM (orange), 8 mM (pink). Inset: corresponding amperograms (E = 0.0 V and t = 300 s) obtained from the detection of H_2O_2 enzymatic by-product in absence (black) and in presence of SM concentrations equal to 2 mM and 4 mM. **B)** Inhibition percentage values (n = 3) for increasing concentrations of aerosolised SM: 0.019 g/m^3 (light blue), 0.19 g/m^3 (red), 0.76 g/m^3 (green), calculated from current values sampled at different time of measurement: 180 (●) 240 (▼) and 300 (■) s. Inset: corresponding amperograms (E = 0.0 V and t = 300 s) obtained from the detection of H_2O_2 enzymatic by-product in absence (black line) and in presence of SM concentrations equal to 0.019 g/m^3 and 0.76 g/m^3. Measurements were carried out in a mixture of phosphate buffer 50 mM + KCl 0.1 M (pH = 7.4) and ethanol at 5% v/v (A) and 2.5% v/v (B). (For interpretation of the references to color in this figure legend, the reader is referred to the web version of this article).

3.6. Origami-ePAD: stability and selectivity

The origami-ePAD stability over the time was evaluated by storing the devices in controlled conditions after the reagent pre-loading. Since the stability of enzymatic biosensor is usually dependent on the enzyme stability, this key aspect has been already studied in the previous work (Colozza et al., 2018) by maintaining the enzyme solution at 4 °C up to 7 days, observing a good stability of the enzyme. In the present work, we studied the stability of origami-ePADs stored both at room temperature (between 22 and 25 °C) and at 4 °C up to 7 days. The resulting amperometric responses (Fig. S2A) highlighted a slight decrease of the enzymatic activity after 12 h and 24 h (around 20% of decrease), while higher decrease occurred after 72 h (around 40% of decrease) and 168 h (around 60% of decrease). No significant difference between the two storage temperatures was observed. These results showed that the developed origami-ePADs can be used within 24 h after the pre-loading of the enzyme and the substrate.

Also the specificity of the origami-ePAD was investigated. Since the detection is based on the monitoring of ChOx enzymatic activity, an intrinsic selectivity is already provided by the selectivity of the enzymatic reaction itself. However, possible interferences can be caused by other inhibitors that can be found in the battlefield, such as other kinds of chemical warfare agents or secondary products derived from the use of firearms and bombs. For these reasons, we tested the origami-ePAD response in presence of three substances: paraoxon (POX), which is a simulant of another kind of chemical weapons, namely nerve agents; As^{3+}, which can be found as a by-product of arsenic-based chemical weapons (i.e. arsine, Lewisite); Pb^{2+}, which can be released into the environment from the use of firearms and bombs. Such substances can be found in the battlefield at a trace level, and represent possible enzyme inhibitors. In detail, the origami-ePAD response was tested in presence of 150 ppb of each of substances, corresponding to the micromolar level. In addition, taking into account that different chemical warfare agents can be used simultaneously, the effect of POX was studied also at concentration of 150 ppm (0.5 mM), with the aim to evaluate the effect of nerve agent simulant using a concentration comparable with the range studied for mustard agents. The results (Fig. S2B) showed that the origami-ePAD response was slightly affected by the tested substances. More precisely, the enzymatic activity underwent an inhibition of 35% in the case of As^{3+}, and lower than 20% in the case of POX at both ppb and ppm levels, while the presence of Pb^{2+} did not cause appreciable inhibition. This study confirmed the affordability of the developed origami-ePAD for the in-field monitoring of MAs.

4. Conclusions

Herein, the first origami-inspired paper-based electrochemical biosensor for MAs detection was developed. Such miniaturised ePAD was designed for the measurement of MAs both in the liquid and aerosol phase, with LOD equal to 1 mM and 0.019 g/m^3, respectively. The use of filter paper as support of the ePAD allowed to pre-integrate the reagents into the origami layers, obtaining a regent-free biosensor which represents one among the few examples of paper-based wearable electrochemical sensor developed for application in the security field. In particular, it meets many of the requirements needed for the development of easy/ready-to-use and portable devices, resulting in a suitable analytical tool for the on-site detection of MAs as well as for the realisation of rapid and wearable alarm systems to be applied in the high-risk zones. In detail, the wearability of such sensors allow for its integration into portable monitoring devices, drones, or military uniforms. It is worthy to highlight that the analytical approach shown herein could represent a vitally important strategy applicable for the real-time monitoring of a variety of chemical weapon threats, since it can favour early medical interventions as well as the immediate evacuation of affected areas.

Credit author statement

All the authors were involved in conceiving the method, designing and performing the experiments, analysing data and writing the paper.

Declaration of interests

None.

CRediT authorship contribution statement

Noemi Colozza: Conceptualization, Data curation, Formal analysis, Investigation, Writing - original draft, Resources, Writing - review & editing. **Kai Kehe:** Supervision, Writing - review & editing, Resources. **Giulio Dionisi:** Investigation, Writing - review & editing. **Tanja Popp:** Investigation, Writing - review & editing. **Amelie Tsoutsoulopoulos:** Investigation, Writing - review & editing. **Dirk Steinritz:** Supervision, Writing - review & editing, Resources. **Danila Moscone:** Supervision, Writing - review & editing, Resources. **Fabiana Arduini:** Conceptualization, Data curation, Formal analysis, Investigation, Writing - original draft, Resources, Writing - review & editing.

Appendix A. Supporting information

Supplementary data associated with this article can be found in the online version at https://doi.org/10.1016/j.bios.2019.01.002.

References

Abe, K., Suzuki, K., Citterio, D., 2008. Anal. Chem. 80 (18), 6928–6934.
Adkins, J.A., Henry, C.S., 2015. Anal. Chim. Acta 891, 247–254.
Anderson, J.S., 1942. CDRE Report No. 241.
Arduini, F., Cinti, S., Scognamiglio, V., Moscone, D., 2017. Paper-based electrochemical devices in biomedical field: recent advances and perspectives. In: Palchetti, I., Hansen, P.D., Barcelo, D. (Eds.), Past, Present and Future Challenges of Biosensors and Bioanalytical Tools in Analytical Chemistry: A Tribute to Professor Marco Mascini 77. Elsevier, pp. 385.
Arduini, F., Cinti, S., Caratelli, V., Amendola, L., Palleschi, G., Moscone, D., 2018. Biosens. Bioelectron.
Arduini, F., Scognamiglio, V., Covaia, C., Amine, A., Moscone, D., Palleschi, G., 2015. Sensors 15 (2), 4353–4367.
Bandodkar, A.J., Jeerapan, I., Wang, J., 2016. ACS Sensors 1 (5), 464–482.
Bandodkar, A.J., Jia, W., Wang, J., 2015. Electroanalysis 27 (3), 562–572.
Barron, E.G., Bartlett, G.R., Miller, Z.B., 1948a. J. Exp. Med. 87 (6), 489–501.
Barron, E.G., Bartlett, G.R., Miller, Z.B., Meyer, J., Seegmiller, J.E., 1948b. J. Exp. Med. 87 (6), 503–519.
Bunkar, R., Vyas, K.D., Rao, V.K., Kumar, S., Singh, B., Kaushik, M.P., 2010. Sens. Transducers 113 (2), 41.
Cánovas, R., Parrilla, M., Mercier, P., Andrade, F.J., Wang, J., 2016. Adv. Mater. Technol. 1 (5), 1600061.
Cate, D.M., Adkins, J.A., Mettakoonpitak, J., Henry, C.S., 2014. Anal. Chem. 87 (1), 19–41.
Chuang, M.C., Windmiller, J.R., Santhosh, P., Ramírez, G.V., Galik, M., Chou, T.Y., Wang, J., 2010. Electroanalysis 22 (21), 2511–2518.
Cinti, S., Arduini, F., Vellucci, G., Cacciotti, I., Nanni, F., Moscone, D., 2014. Electrochem. Commun. 47, 63–66.
Cinti, S., Minotti, C., Moscone, D., Palleschi, G., Arduini, F., 2017a. Biosens. Bioelectron. 93, 46–51.
Cinti, S., Basso, M., Moscone, D., Arduini, F., 2017b. Anal. Chim. Acta 960, 123–130.
Cinti, S., Talarico, D., Palleschi, G., Moscone, D., Arduini, F., 2016. Anal. Chim. Acta 919, 78–84.
Colozza, N., Kehe, K., Popp, T., Steinritz, D., Moscone, D., Arduini, F., 2018. Environ. Sci. Pollut. Res. https://doi.org/10.1007/s11356-018-2545-6.
Dungchai, W., Chailapakul, O., Henry, C.S., 2011. Analyst 136 (1), 77–82.
Gao, W., Emaminejad, S., Nyein, H.Y.Y., Challa, S., Chen, K., Peck, A., Fahad, H.M., Ota, H., Shiraki, H., Kiriya, D., 2016. Nature 529, 509–514.
Haines, D.D., Fox, S.C., 2014. Forensic Sci. Rev. 26 (2), 97–114.
Hill, H.H., Martin, S.J., 2002. Pure Appl. Chem. 74, 2281–2291.
Kangas, M.J., Burks, R.M., Atwater, J., Lukowicz, R.M., Williams, P., Holmes, A.E., 2017. Crit. Rev. Anal. Chem. 47 (2), 138–153.
Kehe, K., Szinicz, L., 2005. Toxicology 214 (3), 198–209.
Kubesa, O., Morrisey, K., Mathews, S., Proetta, J., Li, C., Skladal, P., Hepel, M., 2014. Med. J. Chem. 3 (3), 916–928.
Kumar, V., Anslyn, E.V., 2013. Chem. Sci. 4 (11), 4292–4297.
Li, W., Qian, D., Wang, Q., Li, Y., Bao, N., Gu, H., Yu, C., 2016. Sens. Actuators B 231, 230–238.
Liana, D.D., Raguse, B., Gooding, J.J., Chow, E., 2012. Sensors 12 (9), 11505–11526.

Liu, H., Crooks, R.M., 2011. J. Am. Chem. Soc. 133 (44), 17564–17566.
Liu, Y., Wang, H., Zhao, W., Zhang, M., Qin, H., Xie, Y., 2018. Sensors 18 (2), 645.
Martinez, A.W., Phillips, S.T., Butte, M.J., Whitesides, G.M., 2007. Angew. Chem. Int. Ed. 46 (8), 1318–1320.
Martinez, A.W., Phillips, S.T., Whitesides, G.M., Carrilho, E., 2010. Anal. Chem. 82, 3–10.
McGill, R.A., Nguyen, V.K., Chung, R., Shaffer, R.E., DiLella, D., Stepnowski, J.L., Dominguez, D., 2000. Sens. Actuators B 65 (1–3), 10–13.
Menger, F.M., Elrington, A.R., 1991. J. Am. Chem. Soc. 113 (25), 9621–9624.
Mishra, R.K., Hubble, L.J., Martín, A., Kumar, R., Barfidokht, A., Kim, J., Wang, J., 2017a. ACS Sens. 2 (4), 553–561.
Mishra, R.K., Martin, A., Nakagawa, T., Barfidokht, A., Lu, X., Sempionatto, J.R., Wang, J., 2018. Biosens. Bioelectron. 101, 227–234.
Mishra, R.K., Mohan, A.V., Soto, F., Chrostowski, R., Wang, J., 2017b. Analyst 142 (6), 918–924.
Nery, E.W., Kubota, L.T., 2013. Anal. Bioanal. Chem. 405 (24), 7573–7595.
Rattanarat, P., Dungchai, W., Cate, D., Volckens, J., Chailapakul, O., Henry, C.S., 2014. Anal. Chem. 86 (7), 3555–3562.
Ricci, F., Palleschi, G., 2005. Biosens. Bioelectron. 21 (3), 389–407.
Roshan, R., Rahnama, P., Ghazanfari, Z., Montazeri, A., Soroush, M.R., Naghizadeh, M.M., Ghazanfari, T., 2013. Health Qual. Life Outcomes 11 (1), 69.
Rowell, M., Kehe, K., Balszuweit, F., Thiermann, H., 2009. Toxicology 263 (1), 9–11.
Shi, Y.B., Xiang, J.J., Feng, O.H., Hu, Z.P., Zhang, H.Q., Guo, J.Y., 2006. J. Phys.: Conf. Ser. 48 (1), 292.
Steinritz, D., Emmler, J., Hintz, M., Worek, F., Kreppel, H., Szinicz, L., Kehe, K., 2007. Life Sci. 80 (24–25), 2199–2201.
Wang, Y., Zang, D., Ge, S., Ge, L., Yu, J., Yan, M., 2013. Electrochim. Acta 107, 147–154.